Materials and Design 187 (2020) 108386

Contents lists available at ScienceDirect

Materials and Design

journal homepage: www.elsevier.com/locate/matdes

Progressive microforming of pin-shaped plunger parts and the grain size effect on its forming quality

Jun-Yuan Zheng [a], S.Q. Shi [a], M.W. Fu [a,b,*]

[a] Department of Mechanical Engineering, The Hong Kong Polytechnic University, Hung Hom, Kowloon, Hong Kong
[b] PolyU Shenzhen Research Institute, No. 18 Yuexing Road, Nanshan District, Shenzhen, PR China

HIGHLIGHTS

- A progressive microforming system directly using sheet metal was developed to fabricate pin-shaped microparts as an alternative of micro-machining.
- The tail-designed plunger parts meet the tolerance requirement, but the flat-designed case does not.
- Experimental and numerical results revealed that shear band prefers to be formed with higher velocity gradient and strain accumulation.
- The surface qualities of fine-grained microparts are acceptable on circular profiles, but undesirable on the end of head feature.

GRAPHICAL ABSTRACT

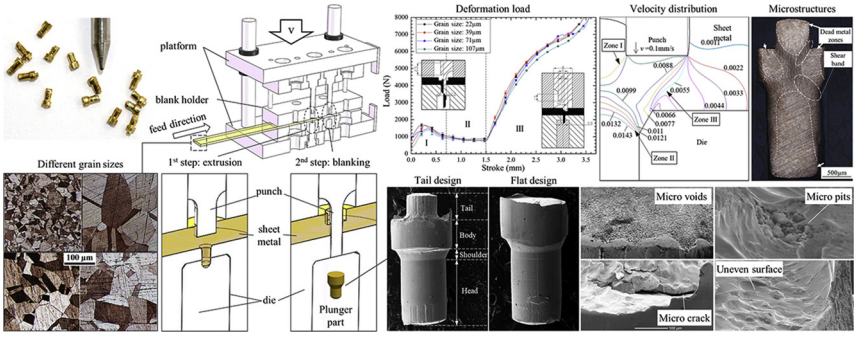

ARTICLE INFO

Article history:
Received 16 September 2019
Received in revised form 11 November 2019
Accepted 22 November 2019
Available online 23 November 2019

Keywords:
Progressive microforming
Grain size effect
Shear band
Forming defects

ABSTRACT

Progressive microforming of bulk microparts by directly using sheet metals has been developed to address the issues of preform/billet positioning, transportation and ejection in microforming, and it has potential to be used for making complex pin-shaped microparts with high productivity and material utilization. In this research, a progressive microforming system with blanking and extrusion operations to make two types of pin-shaped plunger parts by using brass sheets was developed, and the grain size effect was investigated from the aspects of deformation load, dimensional accuracy, microstructural evolution and surface quality. It is revealed that the grain size effect results in the deviation of punch stroke and the variation of part dimension. The formation and characteristics of shear band and dead metal zone are related to velocity gradient and strain accumulation. The forming defects including micro cracks, micro pits, uneven surface and longitudinal surface texture easily occur on the body and tail feature, and micro voids appear with the coarse-grained material. The circular surface, however, shows the desirable quality with each grain size. All these findings provide a basis for mass production of complex pin-shaped microparts by progressive microforming and enrich the knowledges from deformation behavior and product quality assurance aspects.

1. Introduction

The increasing trend of product micromation promotes the demanding for more and more microparts used in electronics, automotive and many other industrial clusters [1,2]. To meet this demand, micro-manufacturing technologies thus emerged in different forms such as

* Corresponding author at: Department of Mechanical Engineering, The Hong Kong Polytechnic University, Hung Hom, Kowloon, Hong Kong.
E-mail address: mmmwfu@polyu.edu.hk (M.W. Fu).

https://doi.org/10.1016/j.matdes.2019.108386

micro-machining, micro-injection, microforming, and micro-assembly [3]. As one of the miniaturized products and a type of micro-connector with good durability and sturdiness, pogo-pin, usually assembled in a plastic housing, is a sort of device widely used in electronics to realize a nonpermanent and flexible electrical connection between two printed circuit boards (PCBs). It is generally comprised of plunger with different designs in the marketplace, barrel and spring in between, as illustrated in Fig. 1. Each part in the assembly of pogo-pin is micropart which has at least two dimensions less than 1 mm. Nowadays, the plunger and barrel parts of pogo-pin are conventionally fabricated by micro-machining, which needs a few time-consuming steps for making different features. Additional machining steps are employed to fabricate multi-features. To meet the required tolerance and quality, many factors should be considered, viz., cutting speed, feed rate, surface finish, and tooling defection, etc. [4]. For microforming, on the other hand, there is no extra forming step but only an improved tooling with suitable geometry required for making complex structures with higher productivity. The forming process is more controllable and the products are more reliable with the same set of tooling. It has thus been proven to be promising for its higher efficiency and material utilization and the good mechanical properties of the final parts [5,6]. To deal with the problems in handling, transporting and ejection of billet/preform/final part in forming process and facilitate the feasible application of microforming in industries, the so-called progressive microforming has been developed and matured, which is a potential method to realize the industrial wide application of microforming for mass production. Many progressive microformed parts were fabricated in the prior researches, such as flanged micropart [7], microchannel [8], micro-pitch [9] and conical micro-part [10]. Progressive microforming, comprised of several forming operations with a given sequence, is to directly employ sheet metals to fabricate bulk microparts by progressive microtools, in such a way one or more specific features of microparts to be made are formed in each progressive forming operation and the complex microparts with various complex miniaturized features are eventually produced. The primary advantages of this process include precise alignment of tooling and workpiece, easy transport of preform to next operation, and efficient ejection of final parts by blanking operation [11]. In this research, the probability of fabrication of pin-shaped parts by using progressive microforming technology was explored and a microforming system aiming at efficiently producing pogo-pin was developed. By addressing the obstacles in terms of deformation and grain size effect, the in-depth understanding and the scientific insight into the process was developed.

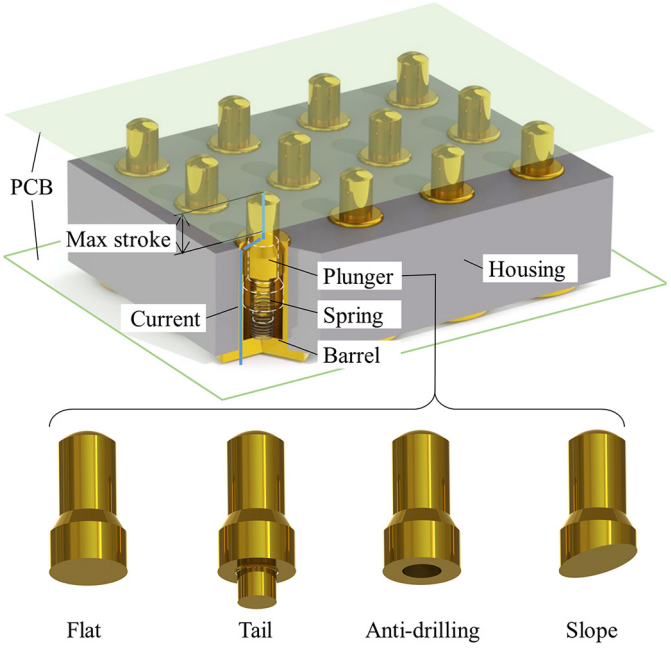

Fig. 1. The structure of pogo-pins.

In the downscaled microforming process, the experience and knowledge developed in macro-manufacturing cannot be applied directly due to size effects [12], viz., geometrical, microstructural grain and tribological size effects, etc. Many prior researches and investigations were conducted to study size effects. Previous studies of grain size effect on micro-extrusion revealed that the coarse-grained material induces inhomogeneous shape [11], lower hardness and strength [13,14], and increased friction factor [15,16]. Parasiz et al. [14] indicated when the grain size grows comparably to specimen with feature miniaturization, penetration of the shear deformation and a typical hardening on central regions happen. Jiang et al. [17] studied temperature and grain size influences in micro-compression, they revealed that coarse-grained microstructure promotes the degree of sensitivity to forming temperature. Fang et al. [18] indicated that the fracture mechanism changes from ductile fracture to brittle fracture when the ratio of material thickness to grain size decreases below one. Leu [19] developed a flow stress model to determine micro-scaled tension from macro-scale considering thickness over grain size ratio. Zhao et al. [20] proposed an improved Zerilli-Armstrong model to depict the correlation of grain size and temperature to material deformation. Park et al. [21] revealed that the decreased initial grain size promote dynamic recrystallization behavior which improves the material elongation. Fan et al. [22] studied grain size effect under thermal and electrically-assisted deformation, and found that fine-grained material shows a higher Joule heating temperature since the increased grain boundaries reduce the electrical conductivity of materials. Meng et al. [23] investigated the grain and thickness size effect as well as crystallographic texture on the anisotropy deformation by geometrically scaled-down deep-drawing tests.

The size effect induced issues such as deformation behaviors in microforming and progressive microforming process, as well as surface fracture, undesirable geometries and dimensional accuracy of microparts were studied by many researchers. Fu and Chan [7] developed a progressive forming process for the fabrication of micro- and meso-flanged parts with a central positioning hole employing punching and extrusion operations, and investigated the size effect affected flow stress, material flow behaviors, and geometrical shapes of microparts. Meng et al. [24] fabricated multi-flanged parts with the four-step progressive microforming. The relationship of grain size effect between the undesirable deformation, the dimensional accuracy and the ductile fracture behaviors and the influences of various ductile fracture criteria were systemically discussed. Ghassemail et al. [25] explored the influences of pin aspect ratios and die entrance fillet effect on the pin-plate microparts produced by progressive microforming. Zheng et al. [26] developed a four-step progressive microforming system for making conical flanged parts and studied the geometrical and grain size affected forming process, undesirable deformation, dimensional accuracy and surface defects of the progressively microformed parts. Ran et al. [27] investigated the dead metal zone induced dislocation strengthening effect on progressive microforming and developed a model based on this phenomenon.

Although prior studies on the microforming process and the fabricated microparts were conducted, there is still lack of a thorough investigation onto the progressive microforming of complex pin-shaped microparts. Pin-shaped parts are not only employed as plunger of connector, but also applied in other electronic components. In this research, a progressive microforming system with two operations of blanking and extrusion by directly using sheet metals was developed and two types of pin-shaped microparts with and without tail feature under different grain size conditions were fabricated. The load-stroke curves of the

forming processes with three deformation stages of various microstructure were presented. The grain size effect affected microstructural evolution and dimensional deviation of the microformed microparts were systemically investigated. Finite element method considering grain size effect was also performed to investigate the forming mechanism of shear band. The typical forming defects and fracture on micropart surfaces were observed and their formation was discussed. The surface quality and roughness were studied considering grain size effect. The findings of this research thus enrich the knowledge and understanding of the process to support the design of complex pin-shaped microparts and progressive microforming tooling and promote the wide application of this efficient microforming process as an efficient alternative to replace the conventional micro-machining.

2. Theoretical and constitutive model

To get the mechanical response and performance of the experimental material for numerical analysis, the coupled constitutive model of surface layer model and Hall-Petch relation was developed and formulated by fitting of the experimental data to represent the flow stress of the materials with different grain sizes. The uniaxial tensile tests for brass CuZn35 were conducted to obtain the experimental data for model generation using five repeated tests with the thickness of 1.5 mm and the grain size of 11, 25, 133 μm. The whole experiments followed the standard of ASTM: E8/E8M. In prior studies, the surface layer model was used, which assumes the specimen is comprised of two parts, viz., surface grains, whose properties are rather similar to single crystal, and inner grains, which is polycrystal and grain boundary strengthening theory takes effect [28]. The Hall-Petch relation combined with surface layer model for the flow stress is illustrated by the following equation:

$$\begin{cases} \sigma_s(\varepsilon_p) = m\tau_R(\varepsilon_p) \\ \sigma_i(\varepsilon_p) = M\tau_R(\varepsilon_p) + k(\varepsilon_p)d^{-1/2} \\ \sigma(\varepsilon_p) = \eta\sigma_s(\varepsilon_p) + (1-\eta)\sigma_i(\varepsilon_p) \end{cases} \tag{1}$$

where σ is the flow stress, σ_s and σ_i are the flow stress contributed by surface grains and inner grains, k is a constant with a given strain related to material properties, ε_p is the plastic strain, τ_R is the critical resolved shear stress, m and M are the orientation factor with the value of 2 for single crystal and 3.06 for FCC polycrystal, respectively, η is the fraction of surface grains, and d is the grain size. To determine the coefficients in the above equations, the curve fitting based on the experimental data is conducted. According to the Hall-Petch equation, the flow stress has a linear correlation with the inverse of the square root of grain size when the plastic strain is fixed. As shown in Fig. 2, $M\tau_R$ is established

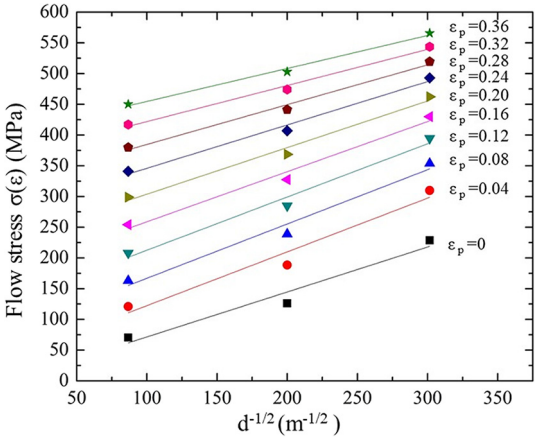

Fig. 2. Flow stress and grain size with the form of Hall-Petch relation of brass CuZn35.

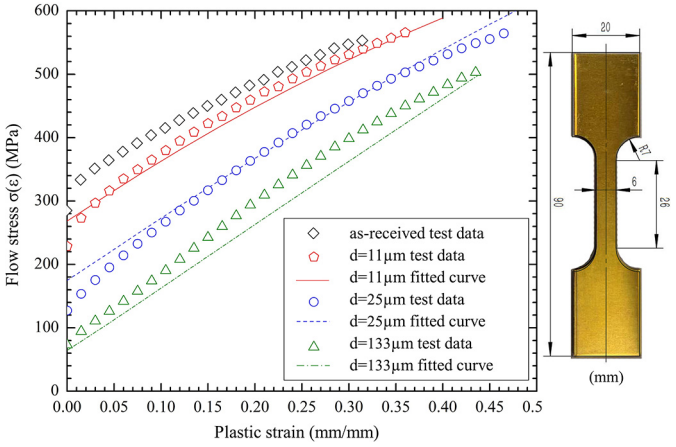

Fig. 3. The fitted and experimental flow stresses with various grain sizes of brass CuZn35.

based on the increments of the fitted linear functions, and k can be obtained based on the slope. τ_R and k can be fitted following the power law function ($y = a + bx^c$) with plastic strain, and the following equations are obtained:

$$\begin{cases} \tau_R(\varepsilon_p) = 388.7{\varepsilon_p}^{1.043} \\ k = 0.903 - 2.162{\varepsilon_p}^{1.705} \end{cases} \tag{2}$$

Then the surface grains are considered to modify the existing model. According to the grain localization model proposed by Lai et al. [29], the fraction of surface grains in sheet materials is determined by $\eta = 2d/t$, where t is the thickness of sheet. By substituting the Eq. (2) into Eq. (1), the final fitted equation for brass CuZn35 is obtained:

$$\begin{aligned} \sigma(\varepsilon_p) = {} & \left(0.903d^{-1/2} + 1189{\varepsilon_p}^{1.043} - 2.162d^{-1/2}{\varepsilon_p}^{1.705}\right) \\ & + \eta\left(-0.903d^{-1/2} - 412{\varepsilon_p}^{1.043} + 2.162d^{-1/2}{\varepsilon_p}^{1.705}\right) \end{aligned} \tag{3}$$

The function curves of Eq. (3) and the related experimental data are illustrated in Fig. 3.

3. Material and experiment

3.1. Experimental material

Brass CuZn35 was selected as the test material due to its wide application in manufacturing pogo-pins and other electronic components for its excellent conductivity and good formability. The brass sheets with the width of 20 mm and the thickness of 2.0 mm were annealed in different temperatures and holding times under an argon-filled furnace to obtain different grain sizes and microstructures, viz. 450 °C for 1 h, 550 °C for 1 h, 600 °C for 1 h, and 750 °C for 1 h, respectively. The solution of 5 g $FeCl_3$, 85 ml H_2O and 15 ml HCl was used as etchant after polishing for etching the cross-section of specimens. The material microstructures along the thickness direction of specimen under different heat treatment conditions are illustrated in Fig. 4(a). The grain sizes were measured based on the lineal intercept procedure of ASTM E112 standard as shown in Table 1.

Table 1
Annealing condition and the corresponding grain sizes.

Temperature (°C)	450	550	600	750
Grain size (μm)	22 ± 4	39 ± 1	71 ± 11	107 ± 15

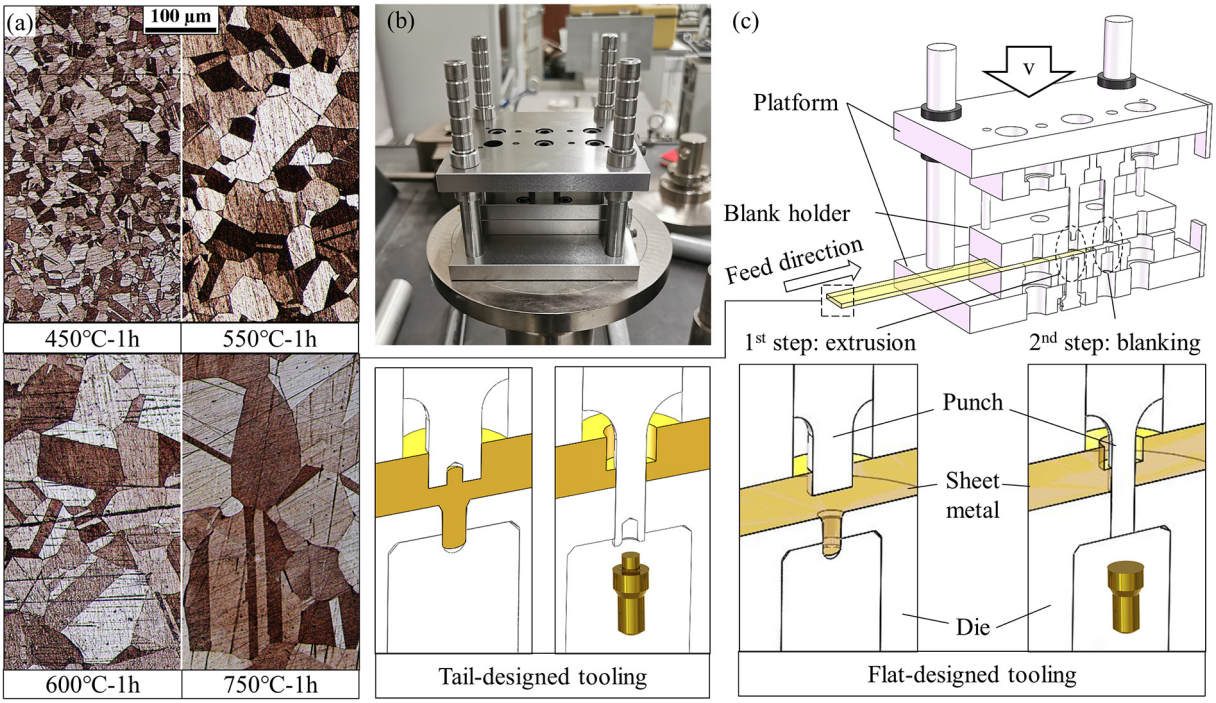

Fig. 4. (a) Initial microstructures of brass sheet under various annealing conditions; (b) The photo of progressive forming system; (c) Illustration of the progressive forming system and forming steps for the two designs.

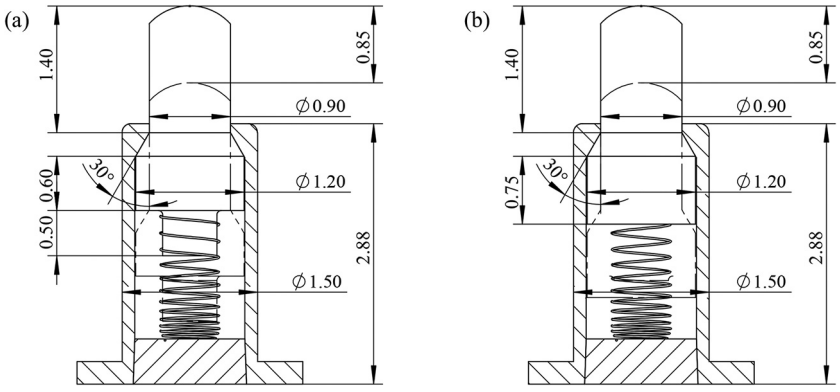

Fig. 5. The dimensions (in mm) of (a) tail-designed and (b) flat-designed pogo-pin assembly.

3.2. Realization of the progressive microforming process

The two structures of the plunger part designed to be formed and their dimensions are shown in Fig. 5. The flat-designed plunger part is the basic design with a simple shape and good formability, but it is instable in lateral direction. The tail-designed plunger part is one of the improved designs to deal with this problem with a good stability. Referring the commercial product (Mill-Max Mfg. Corp.), the tolerances of assembly are ±0.15 mm on length in total and ± 0.051 mm on diameter. For the individual part, the lengthwise tolerance of head feature was thus set as ±0.075 mm and that of the others is not required since it does not affect the total length of assembly. The diametral tolerance of head and body features is ± 0.051 mm. In addition, the surface finish of the plunger part requires 0.5 μm gold over nickel coating. In the relative study [30], the electrodeposited coating thickness is decreased with the increase of surface roughness of substrate. To obtain a desirable coating quality, substrate Ra below 0.4 μm should be employed. The progressive forming system for producing the two plunger parts is illustrated in Fig. 4(c).

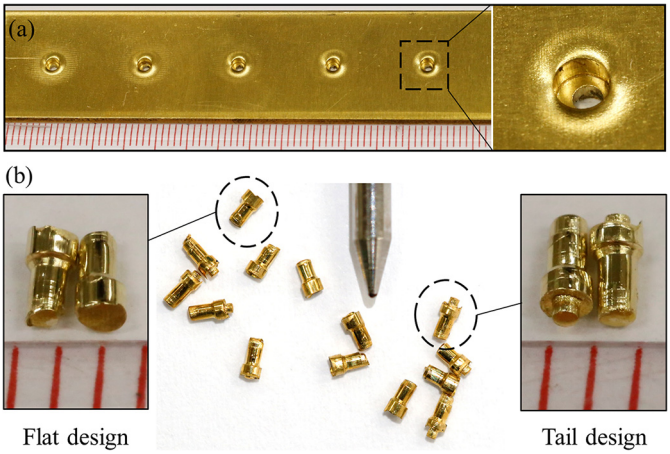

Fig. 6. (a) Sheet metal after forming; (b) The fabricated plunger parts.

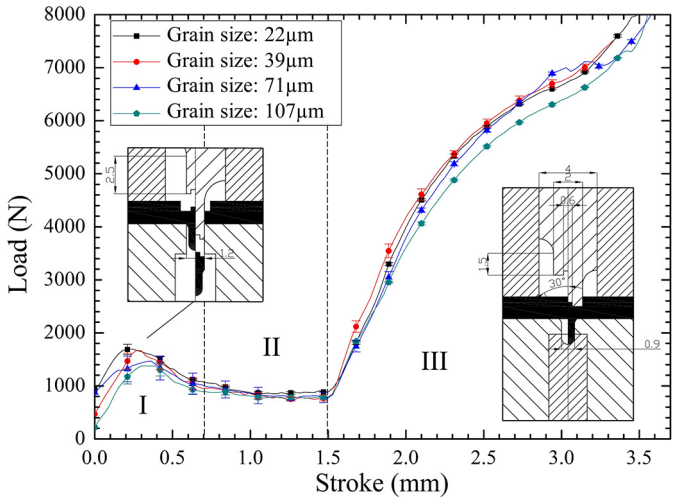

Fig. 7. Load-stroke curves with various grain sizes and tail-designed tooling.

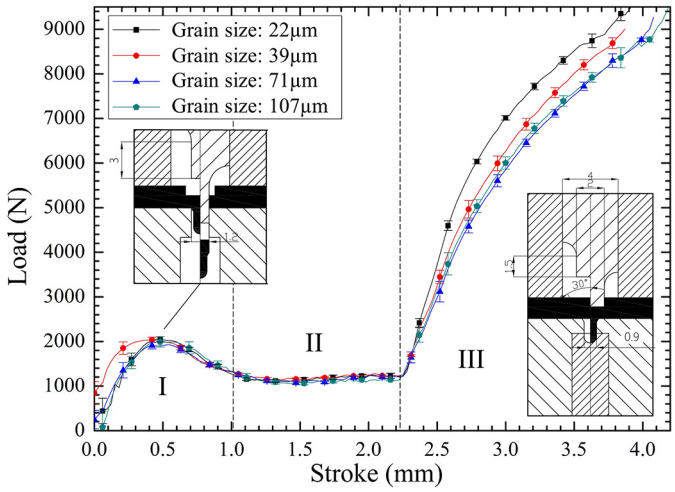

Fig. 8. Load-stroke curves with various grain sizes and flat-designed tooling.

The difference of tooling in design is that the punch for tail-designed plunger has an anti-drilled hole on the tip. This progressive microforming system includes two forming steps, viz., extrusion and blanking. In the first step, the material was extruded into the cavity of punch and die. In the next step, the preformed corner connected to the sheet was used for positioning, and the blank holder was employed to avoid the vertical motion of sheet. After a shearing operation, the plunger part was ejected from the brass sheet. A plunger part was formed and blanked out with a single stroke, and then followed by the release of blanking holder. The brass sheet was moved forward along the feed direction by one step length. After that, the blank holder was screwed, and the next progressive forming process started. The whole progressive forming process was conducted by an MTS testing machine with the maximum load capacity of 50 kN. Machine oil was used as lubricant on each interactive surface among punch, die and specimen in both forming steps. The slow punch velocity of 0.01 mm/s was applied so the strain rate effect could be neglected. The brass sheet after forming and the fabricated microparts are shown in Fig. 6.

4. Results and discussion

4.1. Load-stroke curves in deformation

In microforming process, grain size is one key parameter which influences forming load and stroke, and further affects dimensional accuracy and morphologies of the final parts. The load-stroke relationships with various grain sizes in the forming process of tail-designed plunger scenario and flat-designed plunger scenario are shown in Figs. 7 and 8. The entire forming process in each single stroke of punch is divided into three stages based on the individual progressive microforming operations of blanking and extrusion. At stage I, starting from the blanking punch contacting material and ending by fracture, as the illustration of stage I in the figure, the material is subjected to shearing deformation and the preformed plunger part is then rejected from the brass sheet. It is shown that the ultimate shearing load is decreased with the increasing grain size, which is induced by the reduction of grain boundaries strengthening effect. In the next stage, the forming load shows a stable stage until the extrusion punch contact material. The load in this stage is mainly caused by interfacial friction between tooling and material. Stage III reflects the procedure of extrusion operation, where the material is extruded to preform the head and shoulder features by forward extrusion, and the tail feature by backward extrusion. As the illustration of stage III in the figure. From the load-stroke curves, there is no obvious difference found between these two scenarios. A maximum force limit of the testing machine was settled to control the stroke of upper die in the extrusion operation. When the load exceeds the maximum limit, the vertical stroke is stopped, and one progressive forming process is finished. The maximum limit values were calculated by finite element simulation so that the maximum force of 8000 N was set as the upper limit of the tail-designed scenario while the load of 9500 N was applied for the flat-designed scenario. The diagrams show that the maximum stroke is increased with grain size, which is contributed to the decreasing material strength. The grain size effect on the load-stroke behaviors

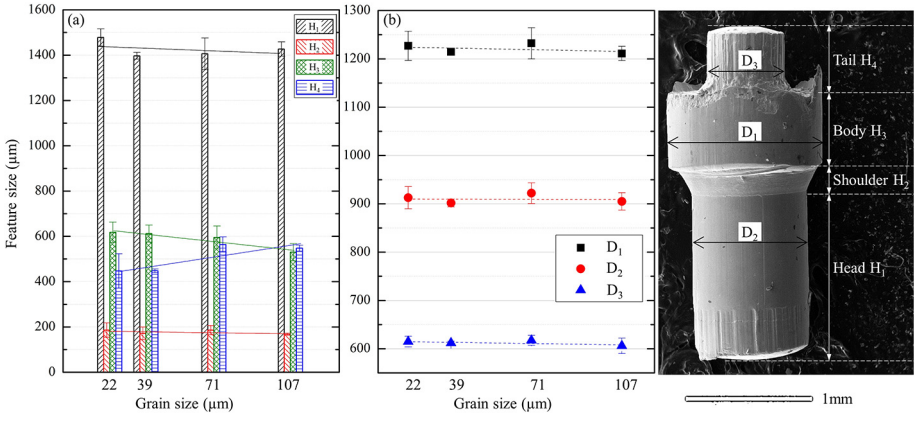

Fig. 9. Lengths and diameters of different features of tail-designed plunger part with different grain sizes.

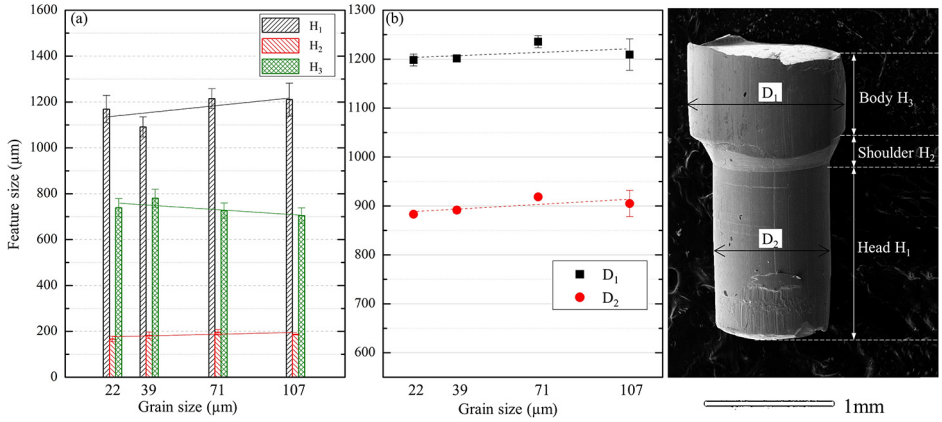

Fig. 10. Lengths and diameters of different features of flat-designed plunger part with different grain sizes.

is related to the characteristic of grain boundary, which acts as a barrier to slip transition. Therefore, when the specimen size keeps steady and the grain size increases, the fraction of grain boundary is reduced, which means the forming load is decreased.

4.2. Dimensional accuracy

Dimensional accuracy of the final parts is one of the key factors to be considered in progressive microforming as it can fully represent the outcome of part design, tooling development and process variable configuration. On the other hand, it is generally affected by tooling manufacturing accuracy, forming operation design, material properties, and the variation of process variables. Compared to macroforming, microforming shows more and severely undesirable phenomena due to its small size scale, worse friction condition and inhomogeneous deformation. To determine the grain size effect on the dimensional accuracy of micro-pin shaped parts, the progressive formed plunger part is characterised by four distinct features, viz., head, shoulder, body and tail, and their lengths are represented by parameters H_1 to H_4, respectively, to clearly elucidate the change of feature dimensions. The diameters of each feature are also represented by D_1 in the body, D_2 in the head, and D_3 in the tail. The lengths and diameters of each feature in the tail-designed and flat-designed parts under different microstructures are summarized in Figs. 9 and 10. It is shown that the length of head feature is slightly diminished in tail-designed parts, varying from 1.478 to 1.397 mm, and almost meets the tolerance requirement (1.4 ± 0.075 mm). But it is decreased from approximate 1.4 mm to 1.2 mm for the flat-designed parts and slightly increased with grain size. It means the flat-designed parts hardly meet the requirement. In contrast to the length, the diameters of each feature in two designs

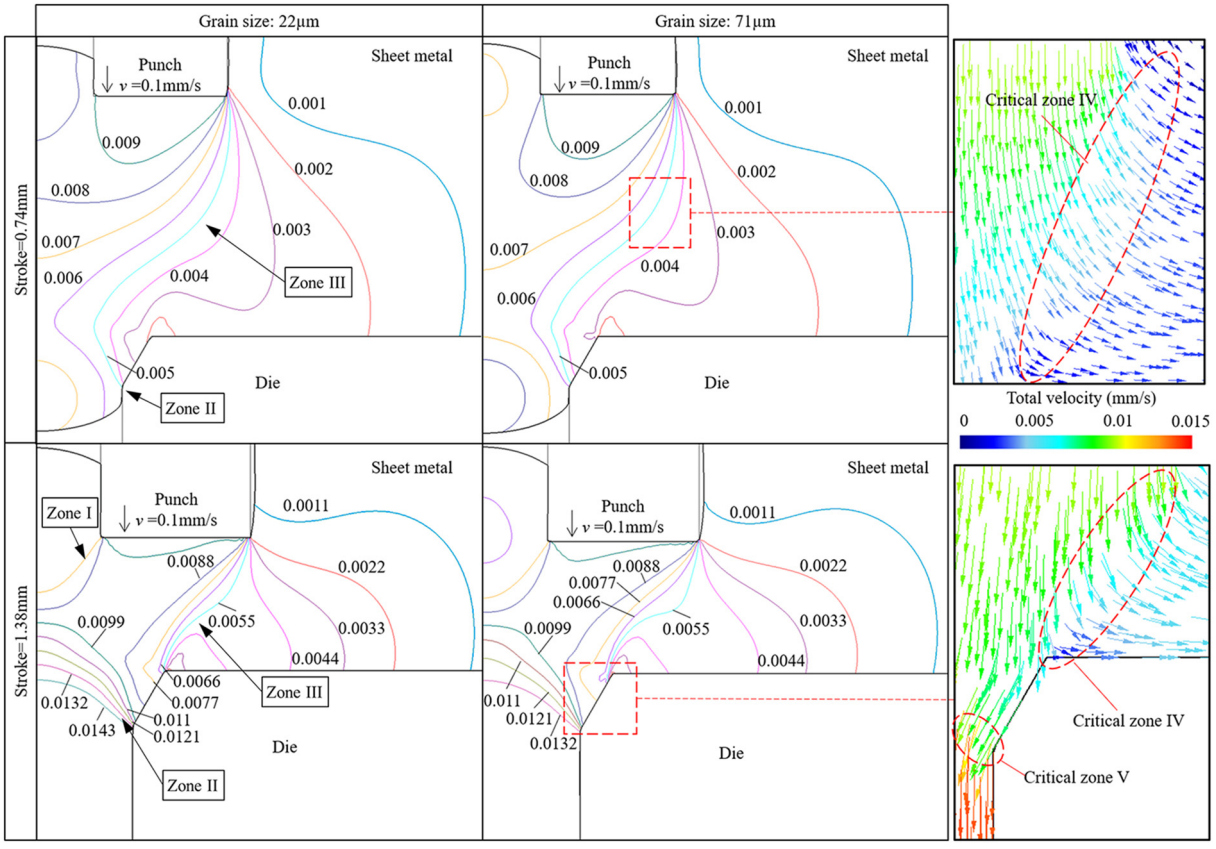

Fig. 11. Material flows (contour and vector) under different strokes and grain sizes.

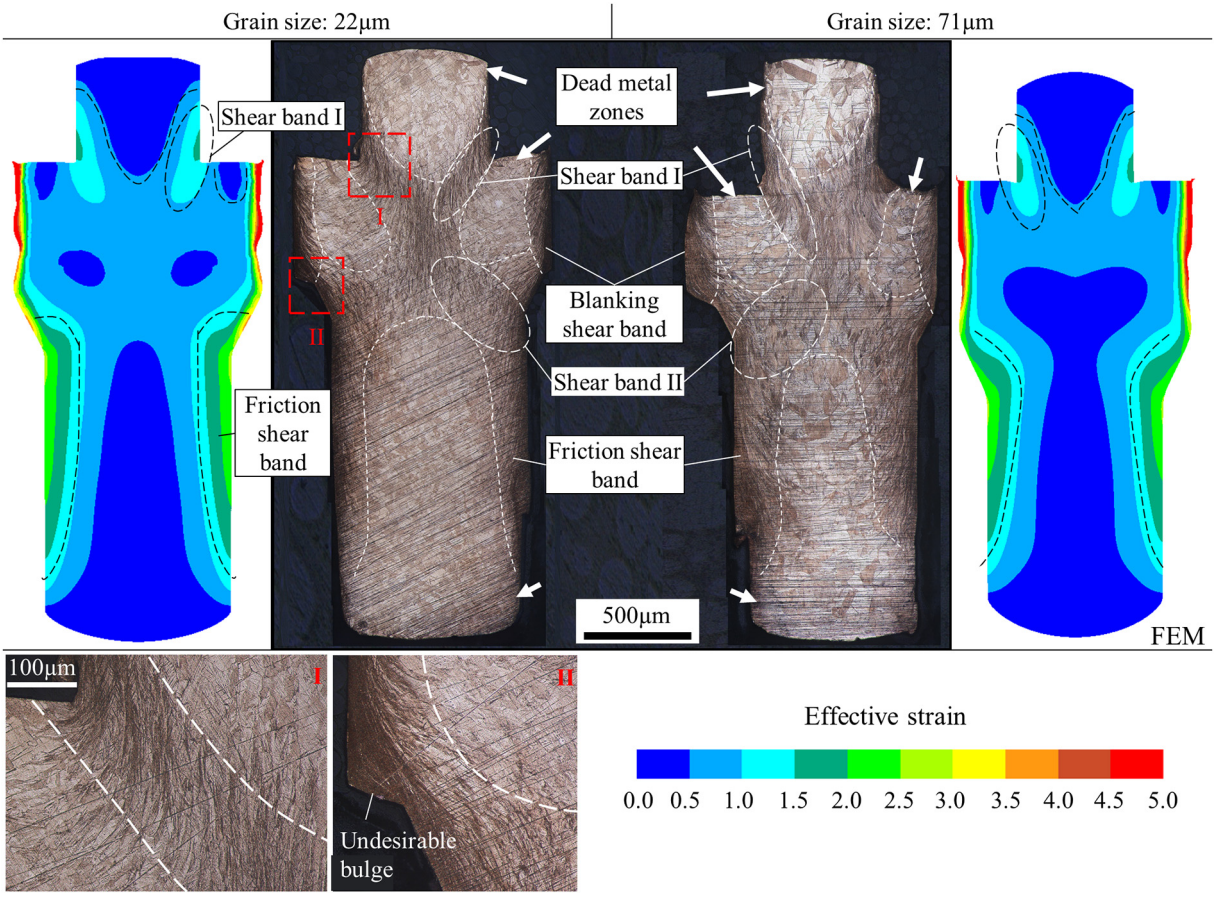

Fig. 12. Microstructures of the cross-section and FEM results of the tail-designed plunger part with the grain size of 22 and 71 μm. (I) The grains in shear band I; and (II) the undesirable bulge.

are not changed a lot and can meet the requirement (±0.051 mm), since it is well constrained by tooling dimensions. Moreover, the length of body feature drops obviously with the increase of grain size for the both designs, which is attributed to the increase of lateral material flow and the reduction of length of extrudate induced by the coarse grain in sheet forming. The length of body feature is easier to meet the designed dimension requirement since it is directly related to the punch stroke. When there are only several grains in the sheet in the thickness direction, the inhomogeneity of grains is increased and thus more materials flow in the unfavorable direction out of punching direction, so that less material remains in the original metal sheet after extrusion operation. In addition, the length of the shoulder feature keeps almost constant since this feature is formed in the middle and is fully constrained by die. Conversely, for the tail-designed parts, the length of tail feature is increased with the growth of grain size, which is the result of the decreasing grain boundary strengthening effect. As the prior studies revealed [16], the grain boundary blocks the slip transferring so that the grain boundary has higher dislocation density and hardness. Therefore, the coarse-grained material with less grain boundaries is softer and easier to be extruded backward. Another factor to be considered is the interfacial friction. Geiger et al. [2] and Engel et al. [31] reported that in combined forward-rod-backward extrusion, the macro-sized coarse-grained specimen tends to flow backward rather than forward compared to fine-grained material due to the friction, but the grain size effect disappears when the billet is scaled down to micro size since the backward flow is limited when the clearance between punch and die is in the order of grain size. In this study, lubricant was employed and the grain size influence on the interfacial friction remains but not significantly since the diameter of tail feature is 600 μm, which is much bigger than the coarse grain size of 107 μm.

4.3. Material flow behaviors

The material flow pattern in progressive microforming is related to the formation of dead metal zones and shear bands. Understanding of the material flow behaviors is important for optimization of the progressive forming process and the properties of the microformed parts. Numerical simulation combined with experiments was employed to study the mechanism of shear band formation. To investigate the mechanism of the formation of shear band, the contour and vector map of material flow with the grain size of 22 and 71 μm in extrusion operation are illustrated in Fig. 11. When the punch stroke is equal to 1.38 mm, there are three zones in sheet metal based on the gradiant of velocity showing the change of material flow velocity. Zone I appears near the inner hole profile of punch; Zone II is from the lower edge of the conical surface of die to the middle; and Zone III appears on the area connected outer profile of punch to the upper edge of the conical surface of die. The velocity gradiant on Zone I is lower than that in other two zones. However, when stroke = 0.74 mm, which is the initial stage of the extrusion operation, Zones II and III can still be observed but Zone I is not clear and even disappears for the fine-grained material. It is revealed that the shear band on Zone I is formed later than Zones II and III during the extrusion. Forcusing on the flow vectors, there is a critical Zone IV appears on Zone III, where the stream of material flow is divided into two directions, viz. longitudinal and lateral. With the movement of punch, the variations of the direction and magnitude of flow velocity in the critical

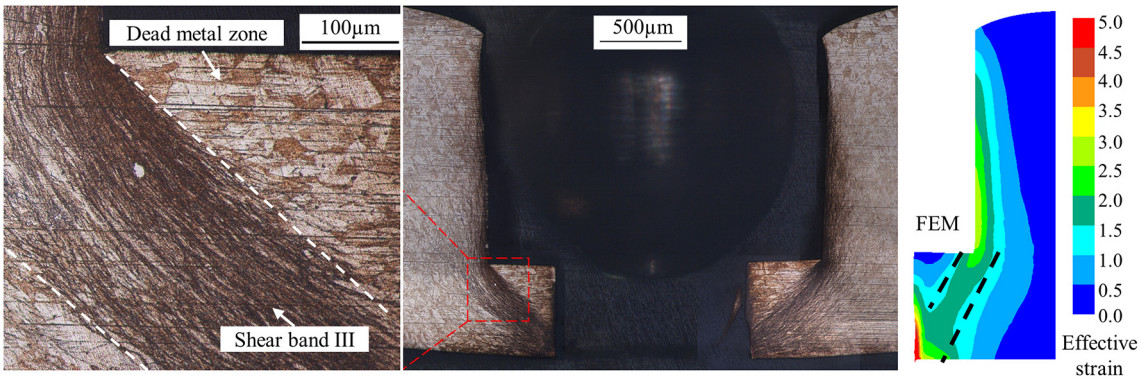

Fig. 13. Microstructures of the cross-section of sheet metal after progressive forming and the FEM result.

Zone IV is significant and a new critical Zone V is formed near Zone II, where the velocity shows an obvious increase and only longitudinal flow remains, which is induced by the reduction of the diameter of die orifice.

Compared to Fig. 12, the microstructures on cross-sections along the symmetric axis of the final tail-designed microparts using the fine-grained material (grain size = 22 μm) and coarse-grained one (grain size = 71 μm) observed by metallographic microscopes, it is revealed that the shear bands are located in Zones I and II. The effective strain distribution shows the formation of shear band I clearly, but shear band II is not. According to Fig. 13, the shear band III induced by Zone III can be found along the corners of punch and die, which is consistent with the effective strain distribution. It is concluded that the shear band prefers to be formed in the area with the large gradient of flow velocity and the area with effective strain accumulation. The shear band I in Fig. 12 shows a decreasing width compared with that in shear band II. Therefore, it can be inferred that the higher gradient of velocity results in a wider shear band. But the variation is not consistent with the effective strain distribution. Moreover, the friction induced shear band in Fig. 12 is not illustrated by velocity change in Fig. 11, but it is precisely calculated based on the effective strain distribution. In addition, on the both sides of body feature, two shearing zones are formed due to blanking operation, which shows the highest strain accumulation in numerical result. The grains in shear band are significantly elongated and distorted along the direction of mateiral flow. From the comparison of different grain-sized material, it is shown that the width of shear band increases with the growth of grain size since a large number of grains are involved in material deformation to share the rotation and elongation at a specific strain, so coarser grains contribute to the larger area of shear band.

Dead metal zone (DMZ) is defined as the place where no or almost no material flow. Prior studies [32–35] of DMZ based on hardness

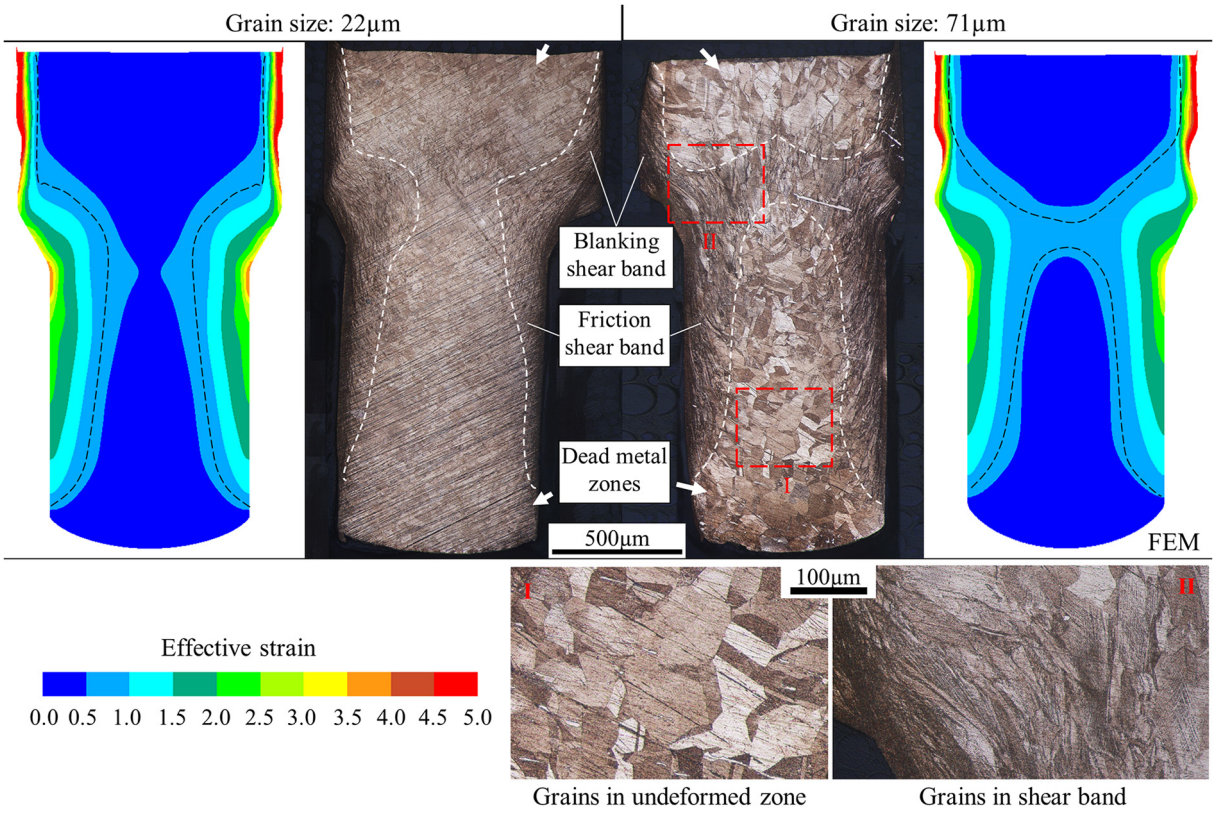

Fig. 14. Microstructures of the cross-section and the FEM results of the tail-designed plunger part with the grain size of 22 and 71 μm. The grains in (I) the shear band, and (II) the undeformed zone.

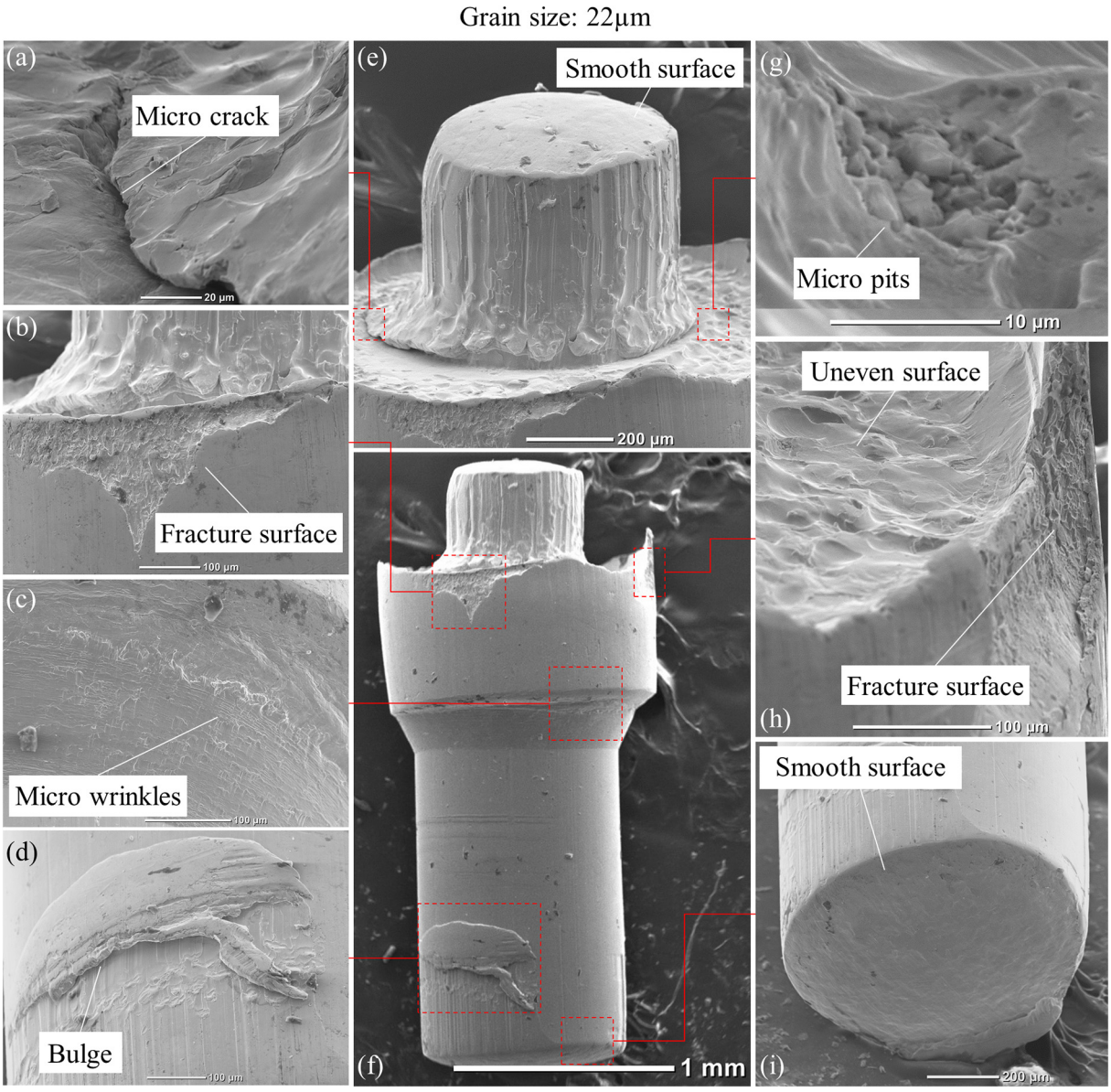

Fig. 15. SEM pictures of the tail-designed plunger part with the grain size of 22 μm.

measurement and flow lines distribution in the etched micrographs showed that the deformation zone morphology is dependent on die geometry, friction, workpiece material, extrusion ratio and loading rate. As shown in Fig. 12, three DMZs are recognized with clear boundaries based on the deformation degree of grains and flow lines. One dead metal zone appears on the top of tail feature with the shape of half round. Two other dead metal zones occur near the top profile of the body feature and they are symmetric with central line. The formation of DMZ is consistent with the fact that DMZ is easily formed underneath the flat indentor in punching, and influenced by the backward extrusion and friction in this scenario, of which the material near the edge of hole is largely deformed and the shear bands are then formed in between the DMZs. In addition, a less deformed zone is formed in the head feature, which is similar to DMZ with negligible straining. In Fig. 13, the microstructure of brass sheet after blanking, two DMZs near the vertical surface of punch and die are shown. Fig. 14 presnets the microstructural evolution of the flat-designed plunger part. The shear band I disappears and the DMZs are connected together. For the coarse-grained material, the shear bands are elongated to the central area. It is verified that the area of shear band is increased with grain size. The formation of shear band is coherent with effective strain distribution.

In summary, shear band prefers to be formed in the area with high gradient of material flow velocity or with the effective strain accumulation. In addition, the wider shear band is reflected by the higher gradient of flow velocity, but not significantly by the effective strain distribution.

4.4. Undesirable geometries

The major undesirable geometry in this progressively microformed part is the deviation of concentricity between the head feature and body feature. As the microstructural images shown in Figs. 12 and 14, undesirable bulge on the side profile appears due to this reason, and the opposite side is thinner. The factor attributing these undesirable geometries is the assembling precision of tooling, interfacial friction, material unfill and the springback of material after extrusion. For design aspect, the corner is designed for positioning, but could cause a deviation in the next blanking operation. Compared with prior researches [26], the corner-based positioning method is not as accuracy as hole-based positioning method. The outer cylindrical surface could be considered for positioning in the future study.

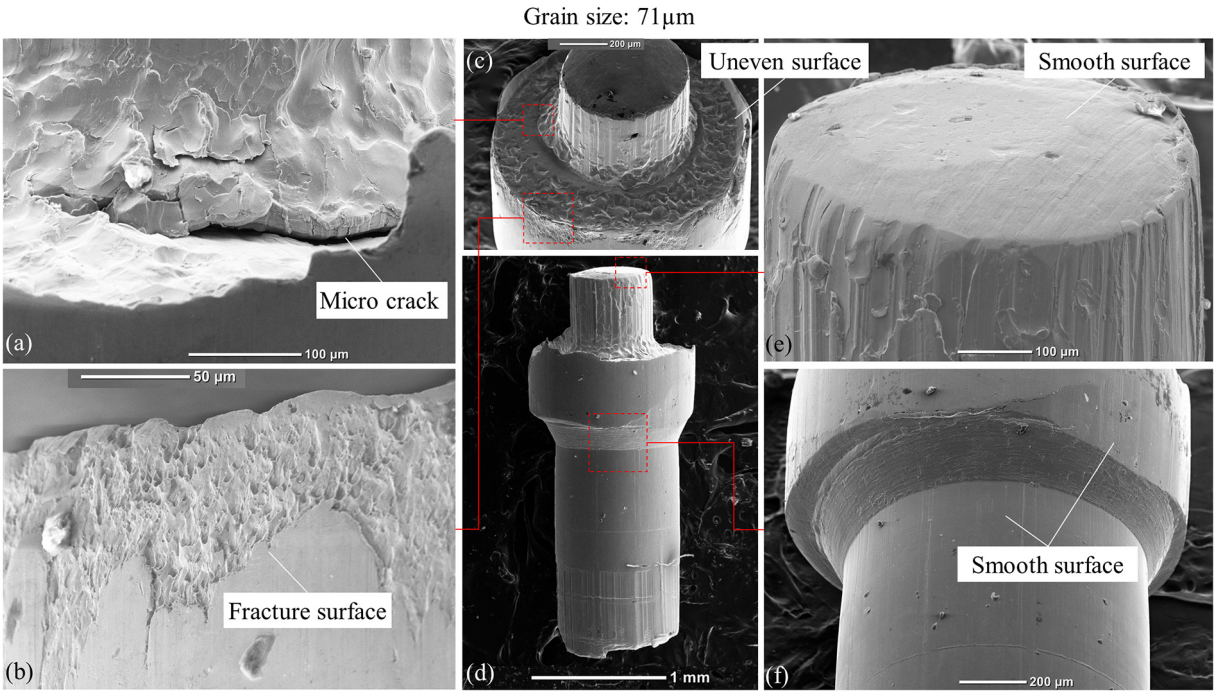

Fig. 16. SEM pictures of the tail-designed plunger part with the grain size of 71 μm.

4.5. Surface fracture

The ductile fracture induced by plastic deformation reaching a certain limit is easier to happen in progressive forming. The morphologies of micro plunger parts in the tail-designed scenario with different grain sizes were observed by Scanning Electron Microscope (SEM) and symmetrically studied. Figs. 15 to 17 illustrate the geometrical shape and defects of the microparts with different grain sizes observed by SEM. As shown in Figs. 15(a), 16(a), and 17(f), micro cracks appear on the edge between tail feature and body feature in all grain sizes, which could be induced by sharp deformation angle and die corner. As prior studies revealed, the sharp corner of die easily causes damage accumulation [25]. Secondary, the top surface of body feature shows an uneven morphology and some micro pits are found on the top surface in Figs. 15

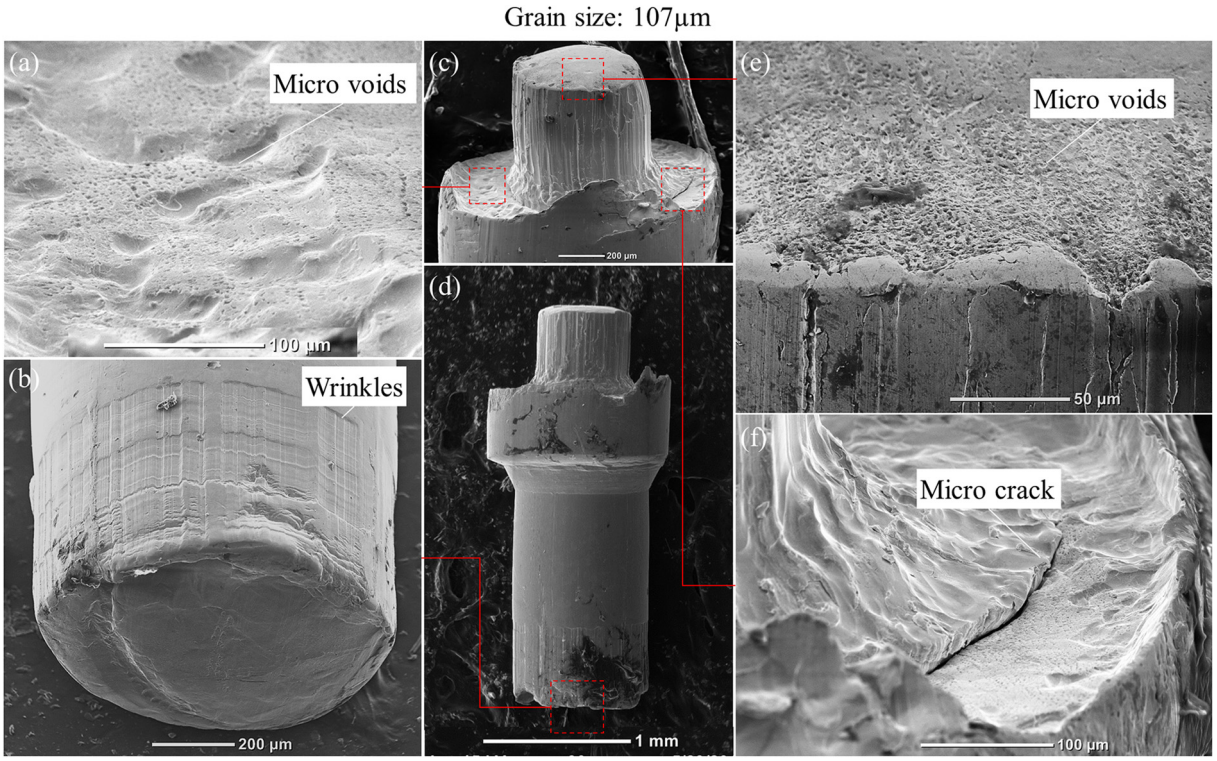

Fig. 17. SEM pictures of the tail-designed plunger part with the grain size of 107 μm.

(g,h), 16(c), and 17(f), which is similar to the phenomena on the large deformed conical surface of the progressively microformed part [26]. Moreover, wrinkles occur on the conical surface of shoulder feature, as shown in Fig. 15(c), where the material flow direction is with 30° to stroke direction. However, micro pits are formed on the largely deformed surface in prior study [26], but on the surface of DMZ in this study. Thus, the forming mechanism of micro pits maybe not so related to the material strain but related to the material flow direction along punch stroke. When the material flow differs from punch stroke, the inhomogeneous deformation and fluctuation away from the desirable material flow direction is easily to occur, which leads to the formation of winkles, micro pits and uneven surface, and the coarse-grained material causes more undesirable geometries. On the other hand, fracture surface and burr appear at the area near the upper edge of body feature and shows randomness, as shown in Figs. 15(b,h) and 16(b), which is a common undesirable geometry appearing after blanking operation [24,26]. The initiating, growing and coalescing of micro voids result in the rough surface and bad surface finish. In addition, as shown in Figs. 15(e), 16(c) and 17(c), the lateral surface of tail feature shows the conspicuous longitudinal surface texture since this surface is backward extruded against to the stroke direction. Compared with the micropart with fine grains, the longitudinal textures on the extrusion surface shows a slight decrease, which could be caused by the decrease of hardness with the larger grains.

Conversely, a smooth surface appears on the profile of head feature as illustrated in Figs. 15(e,f,i) and 16(e,f), since this surface is forwardly extruded to form in parallel to the stroke direction. The surface of body feature is also smooth except for the fracture surface. The desirable smooth surface of head feature facilitates the function of the contact with the barrel of pogo-pin. In addition, the end surface of tail and head features are also smooth since no lateral material flow happens on these two surfaces. The wrinkle or bulge appears near the boundary of two parts of die due to the unperfect contact, as shown in Figs. 15(d) and 17(b).

On the other hand, micro voids are observed on the top surface of body feature and the end surface of the tail feature with the coarse-grained material, as shown in Fig. 17(a,e), but there is no such voids with fine grains. The occurrence of the voids could be caused by the fact of the increasing inhomogeneous deformation in the inherit grains with the larger grain size. This undesirable defect could significantly worsen the performance and durability of the contact surface. It can be predicted that the critical value of grain size that promotes the formation of micro voids falls in between 71 and 107 μm.

Fig. 18 illustrates the variation of surface quality of the top-body, side-body, shoulder, side-head and end of head surface with grain size from 22 to 107 μm of the flat-designed parts. The side-body, shoulder and side-head surfaces show a desirable quality, which are not changed a lot with grain size, especially for the side-head surface, which is contacted by barrel for current flow and requires high wear resistance. However, the top-body surface and the end of head surface are uneven and get worse with the increase of grain size, and with the grain size of 107 μm, voids and crack appear, as illustrated in Fig. 18(a) and (e). The qualities of these two surfaces do not meet the required surface finish, and the subsequent processing such as grinding or polishing process is thus needed to improve the surface quality for the subsequent coating.

In summary, for both two designs, the important side-head surface shows a desirable surface quality, and the wrinkle and bulge can be avoided by a modified die. The end surface of head contact to PCBs in the service environment, so it requires a smooth quality for coating to resist abrasion, therefore, the fine-grained material with a subsequent grinding is preferred. The side-body and shoulder surface show an acceptable quality, but the blanking induced fracture surface should be avoided. Although the side-tail, top-tail and top-body surface show the undesirable unevenness and texture, they are not the contacted surface, so the forming quality is acceptable. The crack on the edge between tail and body feature of the tail-designed parts should be eliminated, which may cause breakage.

4.6. Surface finish

The surface roughness *Ra* is an important factor which can influence the subsequent coating process for the electronic and wear-resistance requirements of the plunger parts. To quantitively study the qualities

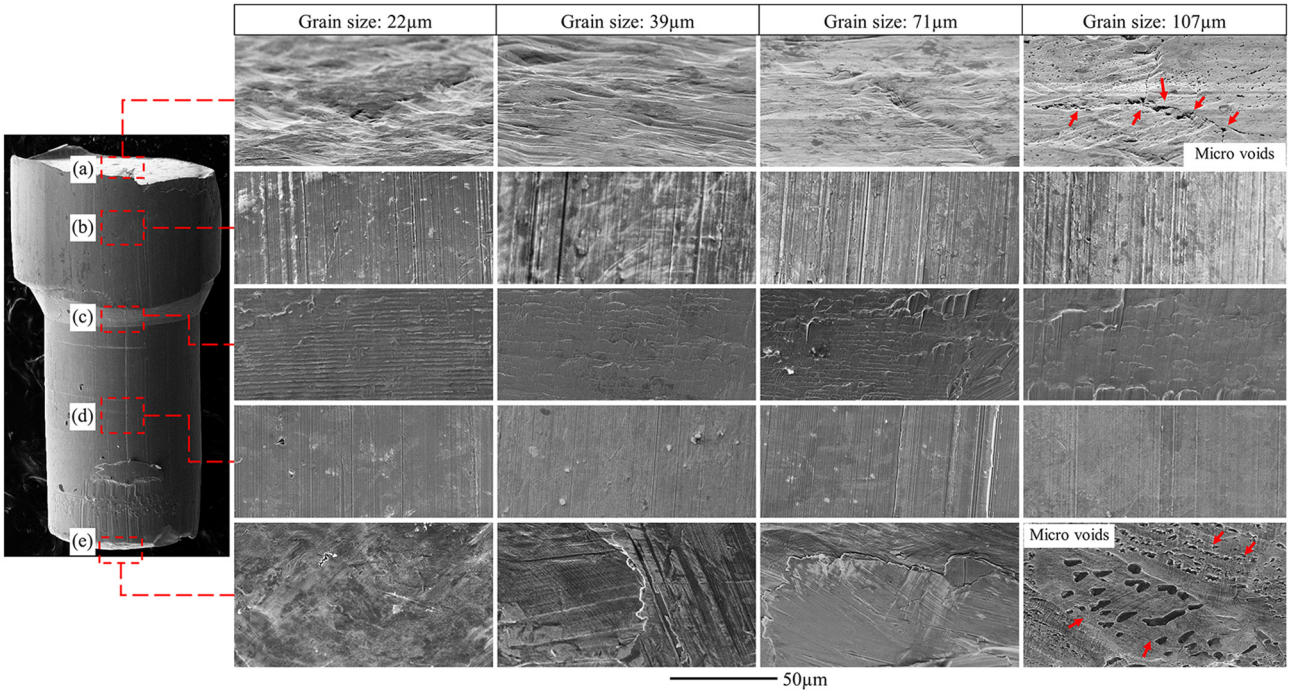

Fig. 18. Morphologies of the surfaces with different grain sizes of the flat-designed part. (a) top-body, (b) side-body, (c) shoulder, (d) side-head and (e) end of head surface.

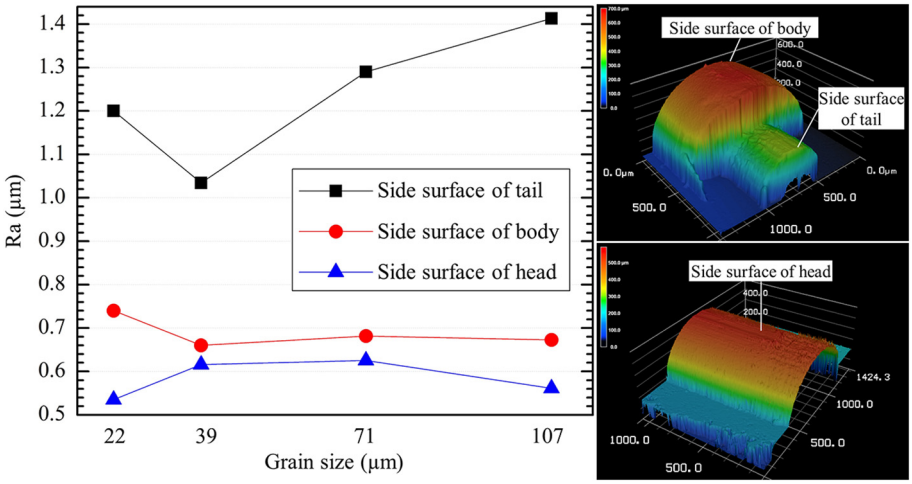

Fig. 19. The surface roughness at the side surfaces of tail-designed plunger parts.

of side surfaces, the surface roughness *Ra* at the side surface of tail, body and head features of the tail-designed plunger parts are illustrated in Fig. 19 measured by 3D laser scanning microscope (Keyence VK-X200). As shown in the diagram, the roughness at the side surface of tail is around 1.0 to 1.4 μm, which is over the roughness requirement, and it shows a rising trend with the increase of grain size. On the other hand, the roughness at the side-head and the side-body surface displays a smoother surface where the roughness is about 0.7 μm of the body and 0.58 μm of the head, and it keeps steady with the change of grain size. Since the same surface on flat-designed plunger parts is formed by the same process, the surface roughness is still referable for the other design. As discussed at the above section, the important side surface of head almost reaches the roughness requirement ($Ra = 0.4$ μm). Therefore, an improved die with high-quality surface finish is required. Moreover, the roughness at the side surface of body and tail is acceptable, and the fine-grained material should be preferred.

5. Conclusions

A progressive forming system was developed for fabrication of pin-shaped plunger part with two design scenarios by directly using sheet metal to replace the traditional micro-machining process. The micro-formed parts were symmetrically investigated from the aspects of microstructural evolution, dimensional accuracy, surface fractures, and the deformation load in forming process considering grain size effect. The following conclusions are thus drawn from this research:

1) The progressive microforming system directly using sheet metals was developed with extrusion and blanking operation, and two types of punch design were employed for different designs of pogo-pin. The forming system can fabricate the plunger part with a single punch stroke, which is an efficient process to produce complex pin-shaped microparts with potential for mass production.
2) With the increase of grain size, the deformation load is decreased, and the punch stroke moves forward. In addition, the height of body feature is decreased, the height of head feature is slightly decreased for tail-designed part and increased for flat-designed part, the height of tail feature is increased, and the height of shoulder feature keeps steady with the increase of material grain size. The diameters of each feature are not changed a lot and meet the design well. The lengths of feature are within the desired tolerance except for the head length of flat-designed plunger part.
3) Shear band prefers to be formed in the area with higher gradient of material flow velocity and effective strain accumulation. In addition, the higher gradient of flow velocity and coarse grains result in a wider shear band formed. Dead metal zones are formed underneath the punch and become small with the coarse-grained material.
4) Strain accumulation induced micro cracks, inhomogeneous deformation induced micro pits, uneven surface and micro winkles, backward material flow induced longitudinal surface texture and unperfect tooling assembling induced bulges and wrinkles are observed as the undesirable defects on the surfaces of microparts. For the grain size of 107 μm, micro voids appear on all the flat surfaces. The side-body, shoulder and tail surfaces show acceptable quality. The roughness of the side-head surface almost meets the requirement.
5) To realize the desirable progressive microforming of the plunger part of pogo-pin, the corner radius of punch and fine-grained material should be considered. The attention should be much paid to assembly precision in such a way to reduce undesirable defects.

For the progressively formed tail-designed pin-shaped microparts with fine-grained brass, its dimensions meet the required accuracy. The side surface of head is close to the ideal roughness, and the surface roughness can be improved by the modified design of die. The forming qualities on other surfaces are acceptable except for the end surface of head feature, which requires a subsequent grinding or polishing. However, the length of head of flat-designed microparts does not meet the tolerance requirement. Therefore, the tail-designed plunger micropart is suggested to be formed by progressive microforming with fine-grained materials.

Declaration of competing interests

The authors declare that they have no known competing financial interests or personal relationships that could have appeared to influence the work reported in this paper.

CRediT authorship contribution statement

Jun-Yuan Zheng: Data curation, Formal analysis, Investigation, Methodology, Software, Visualization, Writing - original draft, Writing - review & editing. **S.Q. Shi:**Resources, Validation. **M.W. Fu:**Conceptualization, Supervision, Writing - review & editing.

Acknowledgements

The authors would like to acknowledge the funding support to this research from the key project of No. 51835011 and the project of No. 51575465 from the National Natural Science Foundation of China, and

the project of 152792/16E (B-Q55M) from the General Research Fund of Hong Kong Government.

Data availability

The raw/processed data required to reproduce these findings cannot be shared at this time as the data also forms part of an ongoing study.

References

[1] U. Engel, R. Eckstein, Microforming - from basic research to its realization, J. Mater. Process. Technol. 125 (2002) 35–44.
[2] M. Geiger, M. Kleiner, R. Eckstein, N. Tiesler, U. Engel, Microforming, Cirp Ann-Manuf Techn 50 (2) (2001) 445–462.
[3] A.R. Razali, Y. Qin, A review on micro-manufacturing, micro-forming and their key issues, Procedia Engineering 53 (2013) 665–672.
[4] B. Boswell, M.N. Islam, I.J. Davies, A review of micro-mechanical cutting, Int. J. Adv. Manuf. Technol. 94 (1–4) (2017) 789–806.
[5] M.W. Fu, J.L. Wang, A.M. Korsunsky, A review of geometrical and microstructural size effects in micro-scale deformation processing of metallic alloy components, Int. J. Mach. Tools Manuf. 109 (2016) 94–125.
[6] M.W. Fu, W.L. Chan, Micro-scaled products development via microforming, Springer Series in Advanced Manufacturing, 10, Springer, London, 2014 , (978-1).
[7] M.W. Fu, W.L. Chan, Micro-scaled progressive forming of bulk micropart via directly using sheet metals, Mater Design 49 (2013) 774–783.
[8] H.-J. Kwon, Y.-P. Jeon, C.-G. Kang, Effect of progressive forming process and processing variables on the formability of aluminium bipolar plate with microchannel, Int. J. Adv. Manuf. Technol. 64 (5–8) (2012) 681–694.
[9] K. Hirota, Y. Watanabe, K. Kuriya, Y. Mori, Improvement of geometric accuracy in progressive slot piercing with small pitch, Procedia Manufacturing 15 (2018) 633–638.
[10] C.J. Wang, L.D. Cheng, Y. Liu, H. Zhang, Y. Wang, D.B. Shan, B. Guo, Research on micro-deep drawing process of concial part with ultra-thin copper foil using multi-layered DLC film-coated die, Int. J. Adv. Manuf. Technol. 100 (1–4) (2018) 569–575.
[11] J. Cao, E. Brinksmeier, M. Fu, R.X. Gao, B. Liang, M. Merklein, M. Schmidt, J. Yanagimoto, Manufacturing of advanced smart tooling for metal forming, CIRP Ann. 68 (2) (2019) 605–628.
[12] F. Vollertsen, D. Biermann, H.N. Hansen, I.S. Jawahir, K. Kuzman, Size effects in manufacturing of metallic components, Cirp Ann-Manuf Techn 58 (2) (2009) 566–587.
[13] S. Nanthakumar, D. Rajenthirakumar, Influence of grain size on deformational behavior in microextrusion process, J. Braz. Soc. Mech. Sci. Eng. 41 (3) (2019).
[14] S.A. Parasız, B.L. Kinsey, N. Mahayatsanun, J. Cao, Effect of specimen size and grain size on deformation in microextrusion, J. Manuf. Process. 13 (2) (2011) 153–159.
[15] C.C. Chang, C.H. Hsu, J.C. Lai, Effects of grain size and lubricating conditions on micro forward and backward hollow extrusion of Brass, Appl. Mech. Mater. 479–480 (2013) 8–12.
[16] W.L. Chan, M.W. Fu, B. Yang, Study of size effect in micro-extrusion process of pure copper, Mater Design 32 (7) (2011) 3772–3782.
[17] Z. Jiang, J. Zhao, H. Lu, D. Wei, K. Manabe, X. Zhao, X. Zhang, D. Wu, Influences of temperature and grain size on the material deformability in microforming process, Int. J. Mater. Form. 10 (5) (2016) 753–764.
[18] Z. Fang, Z. Jiang, X. Wang, C. Zhou, D. Wei, X. Liu, Grain size effect of thickness/average grain size on mechanical behaviour, fracture mechanism and constitutive model for phosphor bronze foil, Int. J. Adv. Manuf. Technol. 79 (9–12) (2015) 1905–1914.
[19] D.-K. Leu, Distinguishing micro-scale from macro-scale tensile flow stress of sheet metals in microforming, Mater Design 87 (2015) 773–779.
[20] R. Zhao, J.Q. Han, B.B. Liu, M. Wan, Interaction of forming temperature and grain size effect in micro/meso-scale plastic deformation of nickel-base superalloy, Mater Design 94 (2016) 195–206.
[21] S.H. Park, J.H. Bae, S.-H. Kim, J. Yoon, B.S. You, Effect of initial grain size on microstructure and mechanical properties of extruded Mg-9Al-0.6Zn alloy, Metall. Mater. Trans. A 46 (12) (2015) 5482–5488.
[22] R. Fan, J. Magargee, P. Hu, J. Cao, Influence of grain size and grain boundaries on the thermal and mechanical behavior of 70/30 brass under electrically-assisted deformation, Mater. Sci. Eng. A 574 (2013) 218–225.
[23] B. Meng, W.H. Wang, Y.Y. Zhang, M. Wan, Size effect on plastic anisotropy in micro-scale deformation of metal foil, J. Mater. Process. Technol. 271 (2019) 46–61.
[24] B. Meng, M.W. Fu, C.M. Fu, K.S. Chen, Ductile fracture and deformation behavior in progressive microforming, Mater Design 83 (2015) 14–25.
[25] E. Ghassemali, A.E.W. Jarfors, M.J. Tan, S.C.V. Lim, On the microstructure of micro-pins manufactured by a novel progressive microforming process, Int. J. Mater. Form. 6 (1) (2013) 65–74.
[26] J.Y. Zheng, H.P. Yang, M.W. Fu, C. Ng, Study on size effect affected progressive microforming of conical flanged parts directly using sheet metals, J. Mater. Process. Technol. 272 (2019) 72–86.
[27] J.Q. Ran, L. Xu, J.L. Wang, T. Xu, F. Gong, Influence of dead metal zone on dislocation strengthening effect during micro-progressive forming, Int. J. Adv. Manuf. Technol. (2019) 1–13.
[28] L. Peng, X. Lai, H.-J. Lee, J.-H. Song, J. Ni, Analysis of micro/mesoscale sheet forming process with uniform size dependent material constitutive model, Mater. Sci. Eng. A 526 (1–2) (2009) 93–99.
[29] X. Lai, L. Peng, P. Hu, S. Lan, J. Ni, Material behavior modelling in micro/meso-scale forming process with considering size/scale effects, Comput. Mater. Sci. 43 (4) (2008) 1003–1009.
[30] A.N.G. Kong, B.-K. Gong, G. Wang, H.-W. Cui, Influence of surface roughness of substrate on the properties of Ni–Co–Fe electrodeposition coating on copper, Surf. Rev. Lett. 25 (8) (2018).
[31] U. Engel, Tribology in microforming, Wear 260 (3) (2006) 265–273.
[32] T.G. Murthy, C. Saldana, M. Hudspeth, R. M'Saoubi, Deformation field heterogeneity in punch indentation, Proc Math Phys Eng Sci 470 (2166) (2014), 20130807.
[33] S.Z. Qamar, Shape complexity, metal flow, and dead metal zone in cold extrusion, Mater. Manuf. Process. 25 (12) (2010) 1454–1461.
[34] N.K. Sundaram, Deformation field in deep flat punch indentation and the persistence of dead-metal zones, Philos. Mag. 98 (25) (2018) 2326–2344.
[35] W. Zhou, J. Lin, T.A. Dean, L. Wang, Analysis and modelling of a novel process for extruding curved metal alloy profiles, Int. J. Mech. Sci. 138–139 (2018) 524–536.